Design and Performance Characteristics of an Experimental Cesium-137 Irradiator to Simulate Internal Radionuclide Dose Rate Patterns

Roger W. Howell, S. Murty Goddu and Dandamudi V. Rao
Department of Radiology, University of Medicine and Dentistry of New Jersey–New Jersey Medical School, Newark, New Jersey

When radionuclides are administered internally, the biological effect can depend on the total absorbed dose and the rate at which it is delivered. A ^{137}Cs irradiator was designed to deliver dose-rate patterns that simulate those encountered in radionuclide therapy. **Methods:** An 18-Ci ^{137}Cs irradiator was fitted with a computer-controlled mercury attenuator that facilitated changes in dose rates as desired. The absorbed dose and dose rates were calibrated with MOSFET dosimeters customized for low dose-rates. **Results:** Initial dose rates ranging from 0.01–30 cGy/hr can be delivered depending on the location of the cage in the irradiator and the thickness of the mercury in the attenuator system. To demonstrate the irradiator system's capability to deliver dose-rate patterns encountered in radionuclide therapy, a simulation was performed where the dose rate initially increased exponentially followed by an exponential decrease in the dose rate. **Conclusion:** The irradiator system is well-suited to expose small animals to any dose-rate pattern, thereby facilitating calibration of biological dosimeters (e.g., cell survival, chromosome aberrations), which can be used to measure the absorbed dose to a target tissue after administration of radionuclides.

Key Words: variable dose rate irradiator; mercury attenuator; biological dosimetry; cesium-137

J Nucl Med 1997; 38:727–730

When radionuclides are administered for diagnostic purposes in nuclear medicine, the absorbed doses received by the critical organs and tissues are usually sufficiently low, so low that the biological effects cannot be measured reliably. In these instances, these doses are appropriate to rely solely on calculated absorbed doses and these doses are sufficient for risk estimations and comparison of the relative merits of different radiopharmaceuticals. However, when radionuclides are administered for therapeutic purposes, or in cases involving accidental ingestion of high levels of radioactivity, dependence on untested absorbed dose calculations can lead to serious errors in predicting the biological consequence of the radiation exposure. Such concerns are particularly relevant to complex biological systems, such as bone marrow. For example, computational bone marrow dosimetry techniques used in radioimmunotherapy have failed to yield a reasonable correlation between absorbed dose and biological response of the marrow. There are several possible reasons for this failure, among them are: (a) underlying assumptions in the absorbed dose calculations, (b) differences in dose rate patterns, (c) prior treatment history and bone marrow reserve, and (d) nonuniform activity distributions in the marrow compartment. These problems are not unique to bone marrow, but can also exist for other organs as well. Hence, in view of the limitations inherent in computational dosimetry, there is a need for reliable biological dosimeters to verify the computational methods.

It is well known that the biological effect of a given radiation insult is highly dependent on the total absorbed dose, dose rate, linear energy transfer (LET) of the radiations, radiosensitivity of the tissue (*1,2*). While the consequences of these variables are well-established for acute and constant chronic radiation exposure conditions (*1–5*), little is known about the role of these variables for exposures involving internal radionuclides. Internal radionuclides are unique in that they deliver radiation exposures at dose rates that vary in time. These variations are usually exponential in nature and are determined by the effective half-time, which in turn is dictated by the physical half-life of the radionuclide and the biological half-time of the radiochemical. Further complications to the dose-rate pattern can emerge when the uptake of the radiochemical by the tissue is slow, followed by a complex multicomponent exponential clearance pattern. Although the total dose delivered to a tissue may be the same, differences in dose-rate patterns from one radiochemical to another can have a major effect on the biological response of the tissue (*6–9*). Such differences cannot always be predicted a priori using computational absorbed dose estimates and extrapolations based on the response to acute and chronic exposure at constant dose rates. Therefore, it is imperative to develop experimental irradiators that are capable of delivering exposures that are similar to those encountered with internal radionuclides and to establish biological endpoints that can serve as dosimeters so that the consequence of different dose-rate patterns on the biological effect can be investigated.

This article describes a custom-designed ^{137}Cs small-animal gamma irradiator that is capable of delivering chronic exposures of low-LET radiation with any desired variable dose-rate pattern encountered with internal radionuclides. This unique custom-designed irradiator can be used to calibrate biological dosimeters that, in turn, can serve as an indirect experimental measurement of the absorbed dose. Such experimental measurements of the absorbed dose can be used to verify the calculated absorbed doses that are presently relied on in internal radionuclide dosimetry. The irradiator will also facilitate improvement of our understanding of the biological effects caused by complex dose-rate patterns and their dependence on initial dose rate, effective half-times, etc. (*8,9*).

MATERIALS AND METHODS

Overview of the Irradiator System

A ^{137}Cs-irradiator coupled to a computer-controlled variable mercury attenuator (Fig. 1) was designed and constructed to irradiate small animals chronically with dose-rate patterns that match those delivered by internal radiochemicals. The system has three major components: (a) ^{137}Cs irradiator, (b) mercury attenu-

Received Jul. 2, 1996; revision accepted Sep. 4, 1996.
For correspondence or reprints contact: Prof. Dandamudi V. Rao, Department of Radiology, UMDNJ–New Jersey Medical School, MSB F-451, 185 South Orange Ave., Newark, NJ 07103.

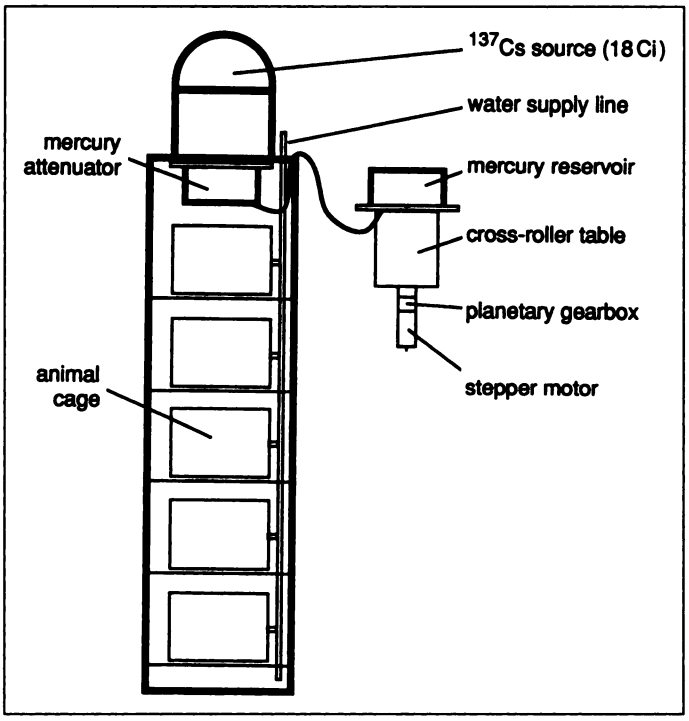

FIGURE 1. Sketch of ^{137}Cs irradiator and mercury attenuator system designed to irradiate animals with exponentially increasing and decreasing dose-rate patterns that simulate those encountered during exposure from incorporated radionuclides.

ator and (c) motion control system. The irradiator delivers low dose-rates of ^{137}Cs gamma rays (0.01–30 cGy/hr) to animal cages housed below the source. The mercury attenuator affords precise control of the dose rate by introducing a layer of highly absorbing mercury between the source and the cages. The liquid properties of mercury allow siphoning of the material between a reservoir outside the irradiator and an attenuation chamber mounted inside the irradiator. A motion control system is used to raise the reservoir to add mercury to the attenuator chamber (i.e., decrease dose rate) and lower the reservoir to remove mercury from the attenuator chamber (i.e., increase dose rate). The computer-controlled motion control system automatically raises and lowers the mercury reservoir to achieve the desired temporal dose rate pattern.

Cesium-137 Irradiator

A low-dose rate ^{137}Cs-irradiator was custom designed for chronic irradiation of small animals (Fig. 2). This self-contained cabinet-like Model JL-28-8 irradiator (inner dimensions 48 × 9 × 13 in.) was constructed by JL Shepherd and Associates (San Fernando, CA). The irradiator houses an 18-Ci ^{137}Cs source that provides a beam of 662-keV gamma rays. The beam is passed through a beam shaper to provide a uniform field. Field uniformity at a distance of 20 cm from the beam port is ±6% over a 6 × 6 in. area. The dimensions of the isodose plane increase as the distance from the beam port is increased. Shelves (1/4 in. lucite) are located within the irradiator that can hold animal cages at different distances below the source, thereby providing different dose rates to each cage. The source-to-cage distances can be varied as desired in 1/4-in. increments. The irradiator is also fitted with a day-night timed light, six-outlet flexible water supply line and a ventilation system to continuously replace the air in the cabinet. In addition, the irradiator has an electronic interlock system to prevent opening of the door during the irradiation.

Mercury Attenuator System

To simulate exponentially decreasing dose rates, a mercury attenuator system was built and coupled to the JL-28-8 irradiator.

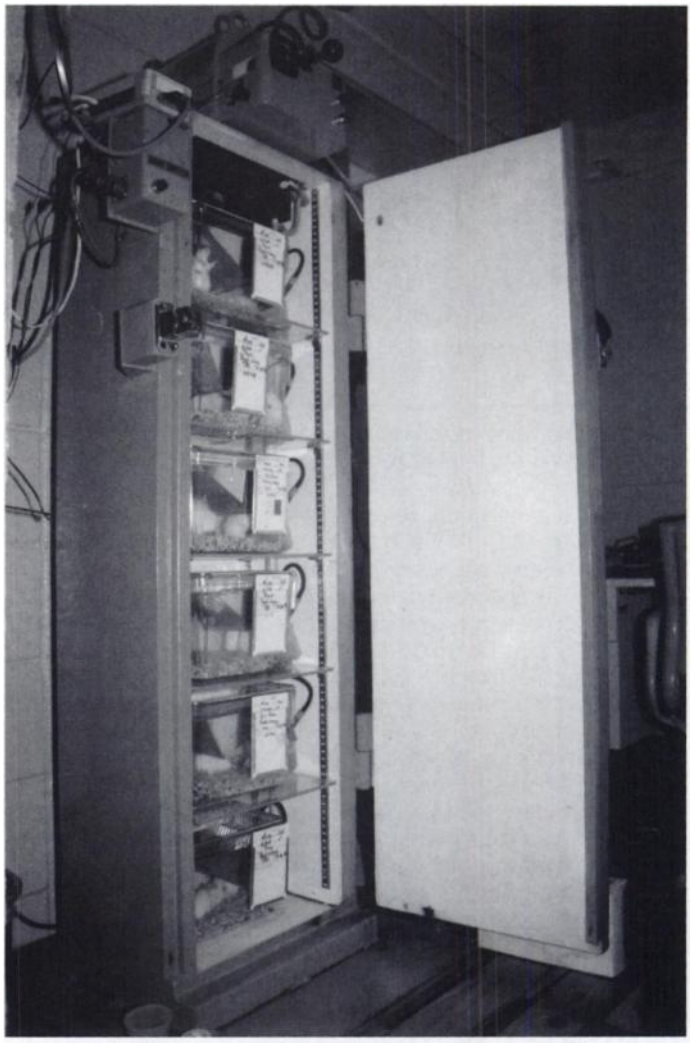

FIGURE 2. Cesium-137 irradiator. Six cages can be placed within the cabinet and irradiated simultaneously, each cage receiving a different dose rate.

The attenuator system consists of two air-tight chambers, the mercury reservoir and the attenuation chamber. The reservoir and attenuation chamber were constructed of 1/2-in-thick clear polyvinyl chloride (CPVC). Holes were drilled and tapped in the bottom of each chamber, and 1/8-in. nylon NPT elbow fittings inserted. The two chambers were then connected with Nalgene reinforced PVC tubing (3/16-in i.d.) to allow transfer of mercury between them. To prevent build-up of air pressure, an additional NPT fitting was inserted into the side of each chamber and connected with Nalgene reinforced PVC tubing to serve as a vent. PVC was chosen for its lack of reactivity with mercury. The attenuator chamber was bolted to the inside of the irradiator chamber between the source and the animal shelves, whereas the reservoir was fixed on a computer controlled platform (Fig. 1). In the absence of air in the mercury transfer line, the mercury thickness in the attenuation chamber depends on the vertical position of the mercury reservoir. Mercury has a linear attenuation coefficient of about 1.49 cm^{-1} for the 662-keV gamma rays of ^{137}Cs. Therefore, a 3.6-cm-thick layer of mercury is expected to attenuate the beam by a factor of about 200. A linear increase in the mercury thickness yields an exponential drop in the dose rate to each animal cage. Therefore, a constant flow rate of mercury into the attenuator chamber provides an exponentially decreasing dose rate to each cage in the irradiator, the half-time of the decrease in dose rate being determined by the flow rate of the mercury. Similarly, a constant flow rate out of the attenuator chamber gives an exponentially increasing dose rate.

Each cage location in the irradiator receives a different initial dose rate depending on the distance from the ^{137}Cs source, however, the dose rates in all of the cages vary with the same half-time. If a multicomponent exponential change in the dose rate is required, the flow rate of the mercury can be automatically altered using the motion control system described below to accommodate the half-time of each component. Finally, the hard limit switches of the Daedal cross-roller table were set to require a mercury thickness of at least 4 mm in the attenuator chamber, the minimum required to cover the entire bottom of the chamber, and a maximum of thickness of 36 mm to prevent overflow into the vent tube.

Motion Control System

The vertical position of the mercury reservoir was automatically controlled using a motorized cross-roller table (Fig. 1). The motorized table consisted of a Daedal (Harrison City, PA) Model 106061C cross-roller table fitted with a Model 04M lead screw (0.4 mm/revolution) and Model 4990-06 z-axis brackets, a Bayside (Port Washington, NY) Model PG60 planetary gearbox with 100:1 ratio and a Compumotor (Rohnert Park, CA) Model 567-102-MO stepper motor. The stepper motor was controlled with a Compumotor Zeta series drive (Model 83-135) and a Compumotor AT6200 two-axis stepper controller housed in a Gateway 2000 386SX/20C computer. The entire system was powered through an American Power Conversion (APC) Back-UPS 1250 uninterruptable power supply. This high precision system, which utilizes a 0.4-mm/revolution lead screw and 100:1 gearbox, increases the mercury thickness in the attenuator by only 2 μm per revolution of the stepper motor.

Software was written in Borland TurboPascal 4.0 to control the motion of the mercury reservoir to provide the desired dose rate pattern, and execute the planned motion by sending Compumotor 6000 Series commands to the motor. The present code can accommodate one-, two- or three-component exponential dose-rate patterns of the following forms. For a single-component exponential,

$$r = r_o e^{-0.693t/T_d}, \qquad \text{Eq. 1}$$

the code requires the decrease half-time T_d (time required for dose rate to decrease to one-half of its value)* and the initial dose rate r_o required for cage Position 1. A two-component exponential dose-rate pattern, where there is an initial period of increasing dose rate followed by a period of decreasing dose rate, is given by (*10*)

$$r = r_o(e^{-0.693t/T_d} - e^{-0.693t/T_i}). \qquad \text{Eq. 2}$$

In this case, the code requires the extrapolated initial dose rate r_o (*10*), increase half-time T_i (time required for dose rate to increase from zero to one-half of r_o) and decrease half-time T_d. Finally, for a three-component pattern that simulates an increase phase and two decrease phases, the dose rate is described by

$$r = r_o\{(ae^{-0.693t/T_{d1}} + (1-a)e^{-0.693t/T_{d2}}) - e^{-0.693t/T_i}\}. \qquad \text{Eq. 3}$$

The extrapolated initial dose rate r_o, increase half-time T_i, and decrease half-times T_{d1} and T_{d2}, and the parameter a are required for the code. Although the present version of the code only allows these dose rate profiles (Eqs. 1–3), it can be revised to accommodate any dose-rate pattern.

*The effective clearance half-lives and effective uptake half-time are generally denoted by T_e and T_{eu}, respectively, which are variables that describe the kinetics of the radionuclide in the source region of interest. In our earlier reports (*8–10*), T_e and T_{eu} were also used to describe dose-rate kinetics. Considering that the dose rate in a given target region can be affected by the cross-dose from radioactivity in nontarget tissues, the notation previously used could lead to confusion. Accordingly, in this article, we have used T_d to represent the half-time for dose-rate decrease and T_i to represent the half-time for dose-rate increase. This notation is reserved for dose-rate kinetics.

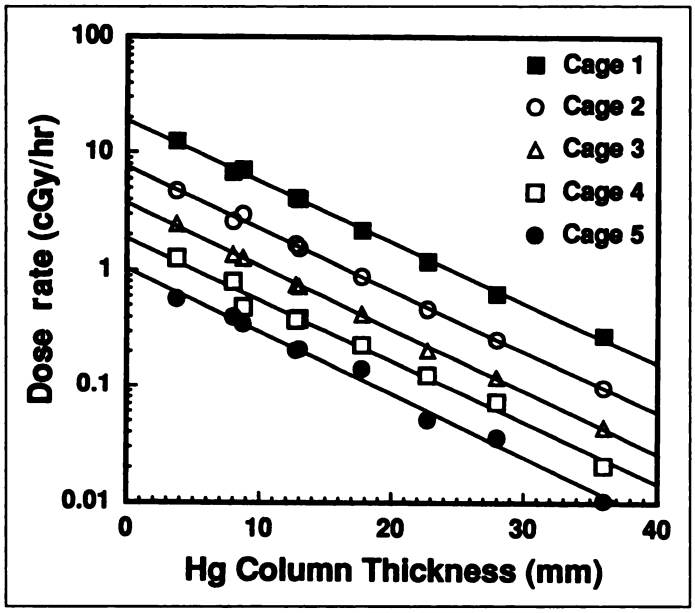

FIGURE 3. Dose rate in mouse phantoms located in Cage 1 (28.6 cm from top of chamber), Cage 2 (48.9 cm), Cage 3 (68.9 cm), Cage 4 (88.9 cm) and Cage 5 (108.6 cm), as a function of mercury thickness in the attenuator chamber.

Calibration

A Thomson-Nielson Model TN-RD-50 MOSFET dosimeter system was used to measure the absorbed dose rate at each cage position in the chamber as a function of mercury thickness in the mercury attenuator chamber. The MOSFET dosimeters and bias power supply were factory customized to allow measurements at low dose rates (<1 cGy/hr) and low doses (as low as 2 cGy). Low doses can be measured with an accuracy of about 10% whereas the accuracy of higher doses (>10 cGy) is within 5%. Dose rates were measured with the probes attached to mouse phantoms placed in the 9 × 6 × 6 in. polycarbonate animals cages (with bedding and wire cage tops). The dosimeter system was also used to monitor the total absorbed dose received by each cage of animals during exposures involving varying dose rates.

RESULTS

The dose rate, as a function of mercury thickness, in the attenuator chamber is given for each cage position in Figure 3. As expected, the dose rate was exponentially dependent on the mercury thickness. Least squares fits of the experimental data for each cage position yielded a mean "effective" attenuation coefficient of 1.22 ± 0.02 cm^{-1}. This value represents the mean slope and s.d. of the curves shown in Figure 3. Given a mercury density of 13.546 g/cm^3, the "effective" mass attenuation coefficient can be calculated to be 0.089 cm^2/g. This value is comparable to the Hubbel's (*11*) theoretical mass attenuation coefficient for mercury of 0.11 cm^2/g for 662-keV photons. Hubbel's theoretical mass attenuation coefficient is expected for a pencil beam. Considering the broad photon beam, the likely contribution of mercury x-rays, and the complex scattering conditions within the irradiator, this 13% difference is not unreasonable.

Figure 3 also shows that the dose-rate changes by a factor of about 20 from the top cage (Cage 1) to the bottom cage (Cage 5) in the irradiator regardless of the mercury thickness in the attenuator chamber. Thus, depending on the cage location and the mercury thickness in the attenuator chamber, dose rates from 0.01 cGy/hr to 12 cGy/hr can be delivered. Furthermore, the maximum dose rate can be increased to as high as about 25 cGy/hr simply by using low-profile (5 cm in height instead of

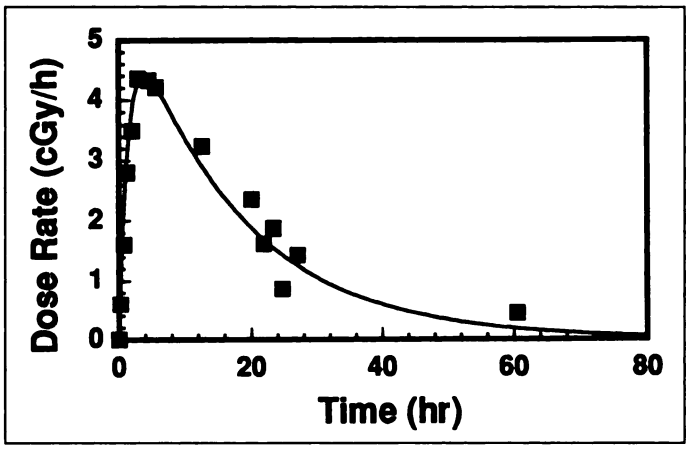

FIGURE 4. Dose rate as a function of time during an irradiation that simulates a two-component exponential dose-rate pattern with a single increase phase (T_i = 1 hr) and a single decrease phase (T_d = 12 hr). The extrapolated initial dose rate was set to 6.0 cGy/hr. The expected dose-rate pattern is represented by the solid line, whereas the experimentally determined dose rates are indicated with the solid squares.

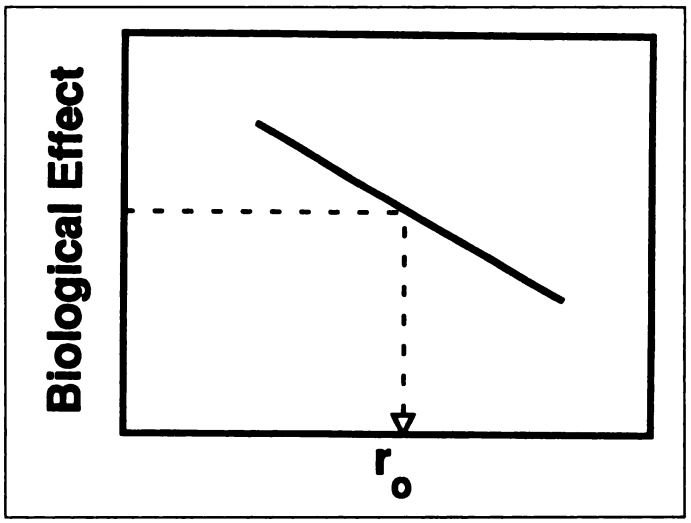

FIGURE 5. Hypothetical calibration curve for an effect (i.e., survival fraction) is given decrease half-time T_d and increase half-time T_i. The biological effect is given as a function of the extrapolated initial dose rate r_o delivered by the ^{137}Cs irradiator. For a given biological effect caused by a radiochemical (same biokinetics parameters), the extrapolated initial dose rate can be determined as indicated by the dashed line.

the standard cage height of 15 cm) animal cages that allow the cages to be placed closer to the ^{137}Cs source.

To demonstrate the capabilities of the irradiator system, a two-component exponential dose rate pattern (Eq. 2) was simulated using a 1-hr increase half-time, a 12-hr decrease half-time, and an extrapolated initial dose rate r_o of 6.0 cGy/hr. Figure 4 shows the resulting experimental dose-rate measurements along with the expected dose-rate pattern based on Equation 2. There is good agreement between the experimental and expected dose rates.

DISCUSSION

The data presented in Figures 3 and 4 show that the ^{137}Cs irradiator and automated mercury attenuator system are capable of delivering dose-rate patterns that are similar to those observed in therapeutic nuclear medicine. Given the strong dependence of biological response on dose rate, this irradiator system is an invaluable tool to assess the biological effects of exponentially varying dose rates on any given target tissue, a largely unexplored area of considerable importance to radioimmunotherapy and other targeted therapies. Caution should be exercised when comparing the biological effects caused by external γ irradiation which delivers the exposure uniformly throughout the tissue and the effects caused by incorporated radionuclides that can lead to nonuniform irradiation of the tissue.

Inasmuch as the relative biological effectiveness of ^{137}Cs 662-keV gamma rays are the same as that of the beta particles emitted by radionuclides relevant to therapeutic nuclear medicine (e.g., ^{90}Y, ^{131}I, ^{32}P, ^{186}Re) (*2*), this irradiator also offers a unique opportunity to calibrate biological dosimeters for bone marrow dosimetry. Examples of potential biological dosimeters include survival of bone marrow subpopulations (e.g., CFU-S, CFU-GM), induction of micronuclei in lymphocytes or reticulocytes, induction of chromosome aberrations in lymphocytes, etc. Calibration of a biological dosimeter to measure absorbed dose delivered to a target tissue by a given radiochemical can be accomplished in two steps:

1. Determine dose-rate kinetics in the target tissue for the radiochemical of interest. When the dose rate to the target tissue is principally due to activity within itself (i.e., self-dose rate), the increase and decrease half-times (T_i, T_d) are essentially equal to the experimentally determined effective uptake half-time T_{eu} and effective clearance half-time T_e of the radioactivity in the tissue. This assumption is generally valid when the primary contribution to the target tissue dose is from particulate radiations (e.g., ^{32}P, ^{90}Y, ^{212}Bi).
2. Using the T_d and T_i established in Step 1, determine the response of the biological dosimeter as a function of extrapolated initial dose rate r_o with the ^{137}Cs irradiator (Fig. 5).

Two additional steps are required to utilize the calibrated biological dosimeter to ascertain the extrapolated initial dose rate received by the tissue after administration of a given activity of the radiochemical:

1. Obtain biological response of tissue after administration of a given activity of the radiochemical.
2. Using the calibration curve, based on the response of the tissue to ^{137}Cs gamma rays delivered with same dose-rate pattern, in other words T_d, T_i (Fig. 5), the extrapolated initial dose rate r_o to the tissue can be extracted. With knowledge of r_o, T_d and T_i, the dose rate and cumulated dose to the tissue can be calculated at any time t.

Calibration and implementation of biological dosimeters in this manner provide an effective means of accurately determining the absorbed dose and dose-rate pattern received by the target tissue after administration of internal radionuclides that emit low-LET radiations. Biological dosimeters calibrated in this manner, however, are not able to provide information regarding dose and dose rate from internal radionuclides that emit high-LET radiations (e.g., alpha particles, Auger electrons). In these situations, the biological dosimeter would yield a quantity that is the product of the relative biological effectiveness and the extrapolated initial dose rate r_o.

CONCLUSION

Internally administered radionuclides irradiate tissue with dose-rate patterns that vary in time. While the biological effects of acute irradiation are well documented, little is known about the effects of time-varying dose rates encountered in diagnostic and therapeutic nuclear medicine. To simulate the irradiation conditions encountered with internal radionuclides, a ^{137}Cs irradiator was custom designed and fitted with a variable

mercury attenuator. This irradiator facilitates the irradiation of small animals with dose rate patterns relevant to internal radionuclides, thereby making it possible to investigate the biological effects of time-varying dose rates and to calibrate biological dosimeters.

ACKNOWLEDGMENTS

We thank the Office of Radiation Safety Services at the University of Medicine and Dentistry of New Jersey for the use of their Thomson-Nielson MOSFET dosimeter system. This work was supported in part by U.S. Public Health Service grant CA-54891.

REFERENCES

1. International Commission on Radiological Protection. *Relative biological effectiveness for deterministic effects.* Publication 58. Oxford, England: Pergamon; 1989.
2. International Commission on Radiological Protection. *1990 recommendations.* Publication 60. Oxford, England: Pergamon; 1991.
3. Testa NG, Hendry JH, Lajtha LG. The response of mouse haemopoietic colony formers to acute or continuous gamma irradiation. *Biomedicine* 1973;19:183–186.
4. Wu C-T, Lajtha LG. Haemopoietic stem-cell kinetics during continuous irradiation. *Int J Radiat Biol* 1975;27:41–50.
5. Thames HD, Withers HR, Peters LJ. Tissue repair capacity and repair kinetics deduced from multifractionated or continuous irradiation regimens with incomplete repair. *Br J Cancer* 1984;49(suppl):263–269.
6. Fowler JF. Radiobiological aspects of low dose rates in radioimmunotherapy. *Int J Radiat Oncol Biol Phys* 1990;18:1261–1269.
7. Langmuir VK, Fowler JF, Knox SJ, Wessels BW, Sutherland RM, Wong JYC. Radiobiology of radiolabeled antibody therapy as applied to tumor dosimetry. *Med Phys* 1993;20:601–610.
8. Rao DV, Howell RW. Time dose fractionation in radioimmunotherapy: implications for selecting radionuclides. *J Nucl Med* 1993;34:1801–1810.
9. Howell RW, Goddu SM, Rao DV. Application of the linear-quadratic model to radioimmunotherapy: further support for the advantage of longer-lived radionuclides. *J Nucl Med* 1994;35:1861–1869.
10. Rao DV, Howell RW. On the modeling of the tumor uptake to determine the time-dose-fractionation effect in radioimmunotherapy [Letter]. *J Nucl Med* 1994;35:1562–1564.
11. Hubbell JH. Photon mass attenuation and energy-absorption coefficients from 1 keV to 20 MeV. *Int J Appl Radiat Isot* 1982;33:1269–1290.

Potential and Limitations of Radioimmunodetection and Radioimmunotherapy with Monoclonal Antibodies

Hui Zhu, Laurence T. Baxter and Rakesh K. Jain

Steele Laboratory, Department of Radiation Oncology, Massachusetts General Hospital and Harvard Medical School, Boston; Radiological Science Program, Massachusetts Institute of Technology, Cambridge, Massachusetts

Recently, we developed a physiologically based pharmacokinetic model capable of predicting antibody biodistribution in humans by scaling up from mice. By applying this model to anticarcinoembryonic antigen murine antibody ZCE025, we address several critical issues in radioimmunodetection and radioimmunotherapy, including the optimal antibody doses, the desirable antibody form for cancer detection, the optimal combinations of antibody forms and radionuclides for cancer treatment and the effectiveness of the modality. **Methods:** Under the baseline conditions of a standard 70-kg man with a 20-g tumor embedded in the liver, the model was used to: (a) estimate absorbed doses in tumor and normal tissues, (b) determine dose-dependent antibody uptake in the tumor, (c) simulate tumor-to-background antibody concentration ratio and (d) calculate therapeutic ratios for different antibody forms and radionuclides. Sensitivity analysis further enabled us to determine antibody delivery barriers and to assess the modality under average and favorable tumor physiological conditions. **Results:** By using ZCE025 under the baseline conditions, the model found that Fab was the most suitable form for cancer diagnosis, while ^{131}I combined with F(ab')$_2$ provided the highest tumor-to-bone marrow therapeutic ratio for cancer treatment. Sensitivity analysis showed that antibody permeability was the major barrier for antibody accretion in tumors. It also demonstrated that normal tissue antigen expression at a level lower than in the tumor had little effect on the therapeutic ratio. **Conclusion:** The model demonstrates that: (a) for radioimmunodetection, the most effective antibody form (Fab for ZCE025) was the lower mol weight form, yet not sensitive enough for hepatic metastasis detection; and (b) for radioimmunotherapy, a relatively fast-clearing antibody form (F(ab')$_2$ for ZCE025) in combination with long half-life β^--emitters was optimal, yet inadequate as the sole therapeutic modality for solid tumors.

Key Words: radioimmunodetection; radioimmunotherapy; antibody pharmacokinetics; mathematical modeling; radiation dosimetry

J Nucl Med 1997; 38:731–741

Received Jan. 3, 1996; revision accepted Apr. 10, 1996.

For correspondence or reprints contact: Rakesh K. Jain, PhD, Steele Laboratory, Department of Radiation Oncology, Massachusetts General Hospital, Boston, MA 02114.

Despite limited clinical success, radioimmunodetection (RAID) and radioimmunotherapy (RAIT) remain potentially useful for cancer diagnosis and treatment (*1–3*). Given the technical challenges and complexity, it is essential to optimize treatment variables to fully realize their clinical potential. Our goal in this investigation was to quantitatively address the following critical issues for RAID and RAIT using anticarcinoembryonic antigen (anti-CEA) murine antibody (ZCE025) as an example: (a) Can absorbed doses be estimated a priori from knowledge of physiological and physicochemical parameters using a mathematical model? (b) What is the relationship between antibody dose and antibody uptake in tumors? (c) What are the optimal antibody doses for a high antibody uptake in tumors? (d) Among the three common antibody forms, IgG, F(ab')$_2$ and Fab, which one is the most suitable for cancer detection? (e) What are the optimal combinations of antibody forms and radionuclides that give high therapeutic ratios based on the biodistribution of antibody and physical properties of radionuclides (radiation emissions and half-life)? and (f) How effective are RAID and RAIT under average and favorable tumor physiological conditions?

Resolving these issues requires extensive clinical pharmacokinetic data under well-controlled conditions. Unfortunately, such data are not available for practical reasons. The use of animal models has allowed researchers to individually assess the roles of antibody dose (*4,5*), antibody form (whole immunoglobulin or fragments) (*6–14*), radionuclide (*15,16*) and tumor physiology (*17*) in RAID and RAIT. However, due to the suboptimal conditions used in these studies and experimental variability, the results are not consistent, and the conclusions are subject to interpretation. A prerequisite for optimally using these preclinical data is the ability to scale up the antibody biodistribution from animals to humans and extrapolate the pharmacokinetics to different treatment variables and physiological conditions. To this end, we have recently developed a